Electronic properties of Ti_3SiC_2-based solid solutions

N. I. Medvedeva
Institute of Solid State Chemistry, Ekaterinburg, Russia

D. L. Novikov
Department of Physics and Astronomy, Northwestern University, Evanston, Illinois 60208-3112

A. L. Ivanovsky and M. V. Kuznetsov
Institute of Solid State Chemistry, Ekaterinburg, Russia

A. J. Freeman
Department of Physics and Astronomy, Northwestern University, Evanston, Illinois 60208-3112

(Received 20 August 1998)

The electronic structure of the silicocarbide Ti_3SiC_2 has been determined by the full-potential linear-muffin-tin-orbital (FLMTO) method. The spectra of the core-electron levels and valence bands of Ti_3SiC_2 have been obtained by x-ray photoelectron spectroscopy (XPS) and compared with the results of FLMTO calculations and x-ray-emission spectroscopy (XES) data. Using XPS data of the inner electron levels (Ti $2p_{3/2}$, Si $2p$, and O $1s$) and the results of band calculations, the nature of chemical bonding in the silicocarbide was analyzed. The high plasticity of Ti_3SiC_2 is explained by a weak interaction between the layers comprising Ti_6C octahedra and plane nets composed of silicon atoms. The electronic and cohesive energy properties of the nonstoichiometric Ti_3SiC and hypothetical Ti_3SiC_2-based solid solutions (SS's), namely Ti_3SiCN and Ti_3SiCO, were simulated by the FLMTO method. An analysis of the cohesive properties shows probable destabilization of the hexagonal structure of Ti_3SiC_2 in the presence of C vacancies and oxygen impurities. By contrast, the partial substitution of N for C ($Ti_3SiC_xN_{1-x}$ SS's) should lead to an increase in the cohesive properties of the crystal. [S0163-1829(98)02148-1]

I. INTRODUCTION

Recently, considerable attention has been devoted to the development of ceramic materials based on silicon and transition-metal (TM) carbides and nitrides, for which there is a great deal of technological interest[1–5] owing to the unique combination of their mechanical, thermomechanical, and electrical resistance properties. For example, silicon-based structural ceramics such as SiC/M and Si_3N_4/M ($M-3d$-$5d$ TM) are promising in machinery as joining and thermistor materials, as coatings for protection against wear and as the materials for microelectronic devices.[1–5]

More complicated ternary phases formed in M-Si-C and M-Si-N systems, the majority of which have the $M_5Si_3(C, N)_x$ composition with the hexagonal Mn_5Si_3-type structure ($D8_8$), are also considered as promising ceramic materials.[6,7] The exception is the Ti-Si-C system, where alongside the $Ti_5Si_3C_x$ phase the high-temperature hexagonal silicon-carbide phase Ti_3SiC_2 (Refs. 8–10) was found by chemical vapor deposition (CVD) and self-propagating high-temperature synthesis (SHS) (Refs. 11 and 12) methods. According to Refs. 6–12, the ternary phase Ti_3SiC_2 has a unique-combination of such properties as resistance to high-temperature oxidation and aggressive environments, high melting point ($t \leqslant 3000\,^{\circ}C$), and plasticlike behavior. Thus, these compounds can be favorably compared to some brittle ceramic materials.

The crystal structure of Ti_3SiC_2 includes layers composed of octahedral Ti_6C groups, the main structural element of cubic binary carbides MC_x.[6] One of the most remarkable features of refractory carbides is their ability to contain considerable concentration of nonmetal lattice vacancies and substitutional impurities (nitrogen, oxygen) when multicomponent solid solutions (carbonitrides, oxycarbides, etc.) are formed. Their appearance may result in quite critical changes in the electronic structure[15,16] and the properties of binary phases.[6,13,14] Thus, we suppose that the above-mentioned disordering effects (in the carbon sublattice) associated with the presence of C vacancies or impurities can take place for the Ti_3SiC_2 phase and will also exert a considerable influence on the electronic properties of titanium siliconitride.

Based on FLMTO calculations we investigated in detail the electronic properties and chemical bonding in Ti_3SiC_2, as well as the possible role of substitutional defects (in the C sublattice) in Ti_3SiC_2-based solid solutions.

II. THEORETICAL AND EXPERIMENTAL METHODS

A. Structures considered and calculational details

According to Ref. 8, Ti_3SiC_2 has a hexagonal structure (space group D_{6h}^4-$P6_3/mmc$) with two formula units per unit cell. The lattice constants are $a = 3.066$ and $c = 17.646$ Å. A fragment of the Ti_3SiC_2 structure is shown in Fig. 1. Titanium atoms occupy two structurally nonequivalent positions, one of which [Ti(1), four atoms per unit cell] has Si atoms as nearest neighbors while the other [Ti(2), two atoms per unit cell] does not. The following interatomic distances[8] (in Å) were used in the calculations:

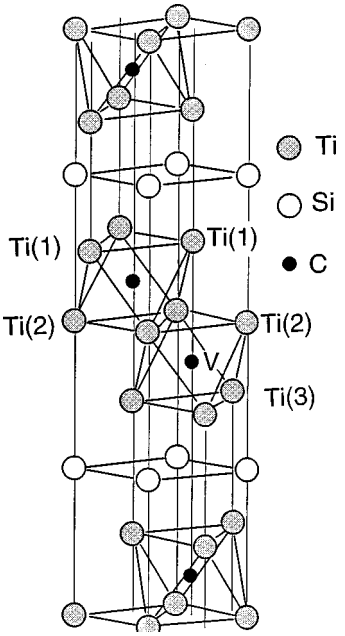

FIG. 1. The crystal structure of Ti_3SiC_2; here Ti(1), Ti(2), and Ti(3) are structurally nonequivalent titanium atoms in Ti_3SiC_2 and Ti_3SiC_2-based solid solutions. ''*V*'' denotes sites of C vacancies or substitutional atoms (N or O) for Ti_3SiCN and Ti_3SiCO.

$$\text{Ti(1)-Ti(1)}=3.068, \quad \text{Ti(2)-Ti(2)}=3.068,$$

$$\text{Ti(1)-Ti(2)}=2.971, \quad \text{Ti(2)-C}=2.135,$$

$$\text{Ti(1)-Si}=2.696, \quad \text{Ti(2)-Si}=2.135,$$

$$\text{Ti(1)-C}=2.135, \quad \text{Si-Si}=3.068.$$

The muffin-tin radii of Ti(1,2), C, and Si were chosen to be 1.92, 2.14, and 2.89 a.u., respectively. The nonstoichiometric silicocarbide (Ti_3SiC) and solid solutions (Ti_3SiCN, Ti_3SiCO) were simulated by substituting one carbon atom (in a unit cell) with a vacancy or with a N or O atom. In this case, there are three nonequivalent types of titanium atoms (Fig. 1). Calculations have also been performed for the hypothetical siliconitride Ti_3SiN_2 with lattice distances obtained by allowing for the differences in atomic radii of carbon and nitrogen.[17]

The FLMTO (Ref. 18) calculations were carried out without any shape approximation to the potential and charge density and with the Hedin-Lundqvist form of the exchange-correlation potential.[19] A triple-κ basis with kinetic energies $k_1=-0.01$, $k_2=-1.0$, and $k_3=-2.3$ Ry was used in the non-spin-polarized calculations. The charge densities in muffin-tin spheres were computed for angular momenta l up to 5, and the Brillouin-zone integrations were carried out using $8\times8\times4$ division in the irreducible part of the Brillouin zone by means of the tetrahedron method.

B. Experiment

In our experiments, we used a specimen of Ti_3SiC_2 prepared by a 20-h sintering of a mixture of TiC, Si, and Ti in vacuum at 1500 K as a result of reaction $2TiC+Ti+Si\rightarrow Ti_3SiC_2$.[22] According to x-ray phase analysis data, this synthesis technique produced single-phase Ti_3SiC_2 with crystal lattice parameters identical to those in Refs. 8 and 9.

XPS measurements were made using the electron spectrometer ''VG ESCALAB MK II'' with x-ray nonmonochromatized Mg $K\alpha_{1,2}$ ($E_\gamma=1253.6$ eV) radiation.

This method was successfully used for investigations of binary TM carbides, nitrides, their solid solutions, and $B1$ thin films TiSiCNO.[20]

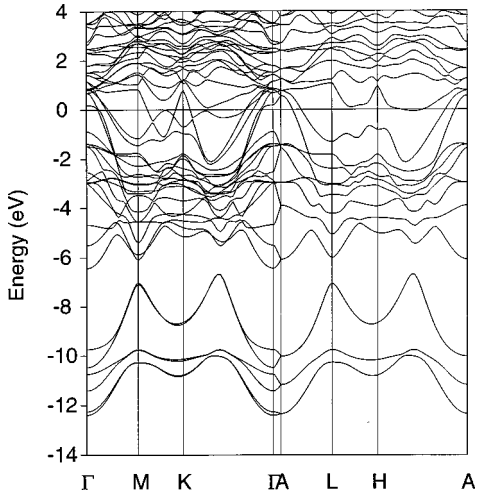

FIG. 2. FLMTO band structure of Ti_3SiC_2.

III. RESULTS AND DISCUSSION

A. Ti_3SiC_2

Figure 2 shows the valence bands of Ti_3SiC_2 as calculated by the FLMTO method. It is seen that the valence bands of Ti_3SiC_2 may be divided into two basic groups: a low-energy group composed of metalloid states mainly of *s* symmetry, and bands containing predominantly valence (Si, C)*p* and Ti 3*d* states. There is no direct overlap of C and Si *s*-like bands (the four lower and the next two bands, Fig. 2). The energy dispersion of the Si bands is larger than for C bands due to the more diffuse character of the 3*s* and 3*p* orbitals of silicon.

TABLE I. Parameters of the band structure of Ti_3SiC_2 and TiC.

		Bandwidth (eV)	Method
	C 2*s*	3.15	
	C 2*p*	4.14	
Ti_3SiC_2	Si 3*s*	4.59	this work
	Si 3*p*	5.05	
	gap (C 2*s*−C 2*p*)	2.79	
	C 2*s*	3.3 (E_F-L_2)	APW (Ref. 24)
	C 2*s*	3.5 (E_F-L_2)	LMTO (Ref. 25)
	C 2*s*	3.9 ($6t_{1u}$-$4t_{2u}$)	DV (Ref. 26)
TiC	C 2*p*	5.6 (L_2'-G_1)	APW (Ref. 24)
	C 2*p*	5.1 (L_2'-G_1)	LMTO (Ref. 25)
	C 2*p*	5.2 ($3a_{1g}$-$6t_{1u}$)	DV (Ref. 26)
	gap (C 2*s*−C 2*p*)	3.2 (L_2-G_1)	APW (Ref. 24)
		3.1 (L_2-G_1)	LMTO (Ref. 25)
		3.5 ($3t_{2u}$-$6t_{1u}$)	DV (Ref. 26)

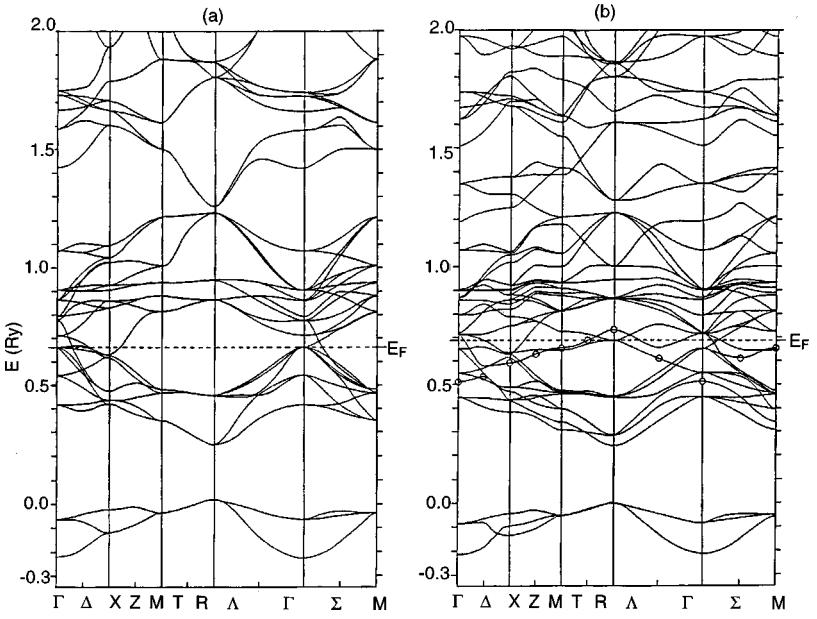

FIG. 3. FLMTO band structure of (a) TiC compared with that for (b) nonstoichiometric $TiC_{0.75}$ from APW calculations (Ref. 54). The bands of ''vacancy'' states are designated by circles.

The energy location and width of C $2s$ and C $2p$ bands are close to those for TiC (Table I). This is in agreement with recent x-ray-emission investigations[23] of Ti_3SiC_2, in which C K_α spectra (C $2p \rightarrow 1s$ transitions) of titanium silicocarbide and titanium monocarbide were found to be similar. However, as distinct from TiC (where the energy gap between s- and p-like bands is ~3.1–3.5 eV) the energy gap between (C,Si) s and (C,Si) p bands of Ti_3SiC_2 is very small: the indirect gap is 0.12 eV and the direct gaps (at the M and L points) are 0.91 and 1.04 eV, respectively.

The Ti valence states in TiC and Ti_3SiC_2 differ considerably, too. For TiC the crystal field splits Ti d states into bonding t_{2g} and antibonding e_g states which overlap insignificantly (cf., Fig. 3). For Ti_3SiC_2 a change both in symmetry and nearest-neighbor composition leads to a substantial overlapping of bonding and antibonding states near E_F (cf., Fig. 2). The largest contribution to this region comes from $3d$ states of Ti(1) atoms located in the vicinity of Si atom layers. The total and local l-projected densities of states (TDOS, LDOS) (Fig. 4) show that for Ti_3SiC_2, the Fermi level (E_F) coincides with the TDOS peak and the DOS at the Fermi level is equal to 4.8 states/eV per unit cell. As a result, the Ti_3SiC_2 phase will exhibit metallic properties, unlike TiC, which is a semimetal. Note that the $N(E_F)$ for TiC does not exceed 0.1–0.5 states/eV unit cell according to various theoretical and experimental estimates.[16,21–26] As pointed out above, for Ti_3SiC_2 the conduction bands near E_F are composed mainly of Ti(1) $3d$ states. Comparing Figs. 4 and 5, where an XPS spectrum of the valence band of Ti_3SiC_2 is shown, one can observe a good agreement between the TDOS and XPS (see also Table II).

Table III presents the total and partial electronic charges inside the muffin-tin (MT) spheres as calculated by the FLMTO method. They show that the main effects of interatomic bonding are due to the participation of metal d and metalloid p states: the occupation of the outer s,p titanium states is low. As regards metalloid s states, the corresponding energy bands do not overlap and are separated from the common p-d valence band by a gap.

It is known (see reviews in Refs. 16 and 27) that the chemical bonding in $B1$ carbides is of a combined covalent-ionic-metallic nature and the covalent component is due to the local interactions of hybridized M d and C $2p$ states. For Ti_3SiC_2, p-d covalent interactions are also retained (Fig. 6). However, as distinct from TiC, for Ti_3SiC_2 individual dd_π-like Ti-Ti bonds for Ti(1) and Ti(2) atoms differ considerably and are much more pronounced for Ti(1) atoms. Figure 7 shows the network of such metallicklike bonds in Ti(1) and Ti(2) planes. The interaction between Ti planes is mediated by hexagonal layers of C and Si atoms. As for TiC, the Ti(1,2)-C interaction in Ti_3SiC_2 of a covalent p-d nature is very strong (Fig. 8), while the Ti(1)-Si interaction is definitely much weaker (Fig. 9). At the same time, Si-Si atoms

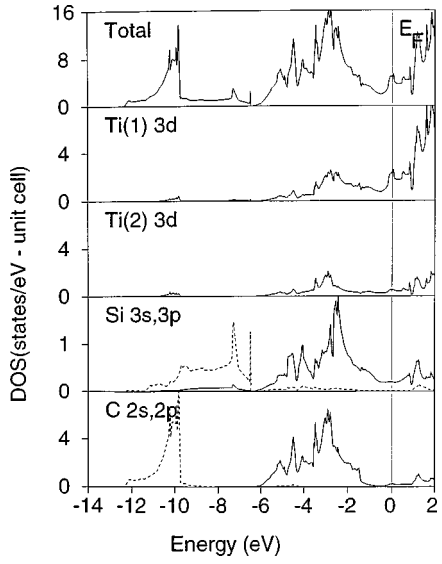

FIG. 4. Total and local densities of states for Ti_3SiC_2.

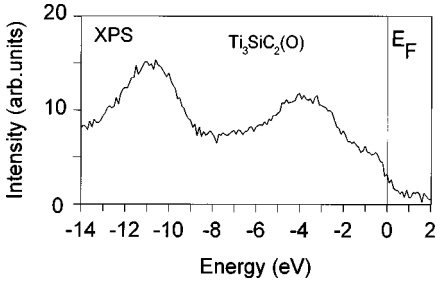

FIG. 5. XPS spectra of valence bands for Ti_3SiC_2.

form a very rigid covalent bond network inside Si monolayers (Fig. 10). This strong anisotropy of chemical bonding is typical for many layered compounds and may qualitatively explain the high plasticity of Ti_3SiC_2-based ceramic materials.[11,12]

These data are in agreement with our XPS results for Ti_3SiC_2 (Fig. 5, Table IV). The binding energies of the core Ti $2p$, Si $2p$, and C $1s$ levels for Ti_3SiC_2 and for a number of silicon and titanium-containing compounds are given in Table IV. Note that the energy locations of the Ti $2p_{3/2}$ and C $1s$ levels (454.8 and 282.1 eV, respectively) for Ti_3SiC_2 coincide with those for TiC and the binding energy of the Si $2p$ level (99.5 eV) is identical to its location in Si bulk. These facts show the similar character of chemical bonding in these compounds and prove the primary localization of Ti bonds to be within the network of Ti_6C clusters. On the other hand, Si bonds are localized within a monolayer forming direct Si-Si bonds.

B. Nonstoichiometric Ti_3SiC

The total (TDOS) and local l-projected density of states (LDOS) of nonstoichiometric (i.e., vacancies in the C lattice) titanium silicocarbide are given in Fig. 10.

It is seen that the removal of some C atoms results in a usual decrease in the widths of the C $2s$ and C $2p$ subbands, which are 1.8 and 3.9 eV for Ti_3SiC as compared to 3.2 and 4.1 eV for Ti_3SiC_2. The energy gap between these bands increases (by $\sim$0.9 eV). At the same time the LDOS of Si $3s$,$3p$ states in the stoichiometric and C-deficient silicocarbides are very close. Consequently, the appearance of C vacancies in Ti_3SiC_x, as in TiC_x, leads to local perturbations of the electronic structure and affects mainly the LDOS distribution of Ti atoms nearest to the vacancy. As noted above, in this case three types of nonequivalent Ti atoms can be distinguished: Ti(1) has C and Si atoms as its nearest neighbors; Ti(2) has C atoms and carbon vacancies (labeled ''V''); and Ti(3) has Si atoms and carbon vacancies (cf. Fig. 1). As seen from Fig. 10, Ti(1) atoms participating in Ti-C and Ti-Si interactions exhibit the strongest bonding with the metalloid sublattice: Ti(2) atoms occupy the intermediate position, and the minimum bonding takes place for Ti(3) atoms (weakly bonded with Si atoms). In the occupied part of the metallic states subband in the region from E_F to -2 eV, Ti(3) atoms have the maximum concentration of electrons and Ti(1) atoms have the minimum concentration. As a consequence, the most pronounced Ti-Ti bonds (dd-type) are formed in the monolayers composed of Ti(3) and Ti(2) atoms; the weak Ti-Ti bonds are formed in Ti(1) monolayers (cf., Figs. 11 and 12).

A decrease in C concentration for Ti_3SiC_x leads [as in the case of TiC_x (Refs. 15 and 16)] to the ''metallization'' of the silicocarbide: $N(E_F)$ increases from 4.8 (Ti_3SiC_2) to 6.8 states/eV per unit cell (Ti_3SiC) (cf., Table V). For the Ti monocarbide,[15,16] C defects result in the formation of ''va-

TABLE II. The energy distance between the centers of the valence bands (eV) of Ti_3SiC_2 according to XPS, XES (taken from Ref. 23), and FLMTO data.

	XPS	XES	FLMTO
E_F-(C $2p$–Ti $3d$–Si $3p$)	4.2		3.9
E_F–C $2s$	10.8		10.2
(C $2p$–Ti $3d$–Si $3p$)–C $2s$	6.6		6.9
(C $2p$–Ti $3d$–Si $3p$)–Si $3s$		5.2	5.4

TABLE III. Total and partial charges in muffin-tin spheres of Ti_3SiC_2- and Ti_3SiC_2-based solid solutions. V s,p,d charge distributions in MT sphere of C vacancies, N, O.

		Ti_3SiC_2	$Ti_3SiC_{1.0}$	Ti_3SiCN	Ti_3SiCO	Ti_3SiN_2
	s	0.089	0.089	0.091	0.092	0.086
Ti(1)	p	0.131	0.133	0.137	0.142	0.133
	d	1.560	1.590	1.584	1.606	1.630
	s	0.091	0.093	0.089	0.086	0.085
Ti(2)	p	0.153	0.126	0.147	0.136	0.141
	d	1.513	1.505	1.517	1.622	1.575
	s		0.105	0.085	0.081	
Ti(3)	p		0.107	0.131	0.120	
	d		1.503	1.621	1.694	
	s	1.485	1.482	1.487	1.421	
C	p	2.782	2.785	2.822	2.683	
	d	0.092	0.098	0.102	0.089	
	s	1.507	1.511	1.509	1.392	1.449
Si	p	2.353	2.307	2.361	2.272	2.243
	d	0.374	0.401	0.444	0.349	0.415
	s		0.692	1.679	1.863	1.682
N,O,V	p		0.197	3.585	4.512	3.625
	d		0.052	0.089	0.104	0.097

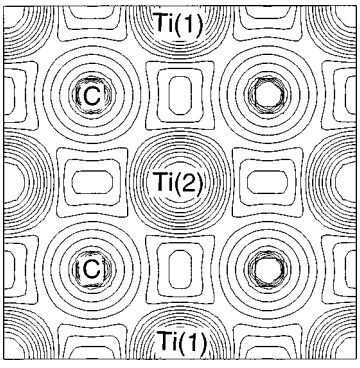

FIG. 6. Valence electron densities in Ti(1)-C-Ti(2)-C-Ti(1) layers of Ti_3SiC_2.

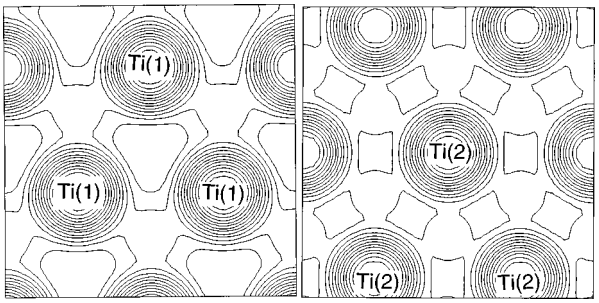

FIG. 7. Valence electron densities in (100)-like monolayers including Ti(1) and Ti(2) atoms of Ti_3SiC_2.

cancy states'' in the vicinity of E_F (Fig. 3). They are formed by Ti d states from broken Ti-C bonds; as a result, $N(E_F)$ increases. For Ti_3SiC_x, the ''vacancy'' states (Fig. 10) are located ~1.7 eV below E_F and the increase in $N(E_F)$ is due to the strengthening in d-d bonding between Ti(2) and Ti(3) atoms.

The bonding properties of Ti_3SiC_2 and Ti_3SiC can be analyzed by comparing their cohesive energies. For this purpose we estimated the values of $E_{\rm dif}=(E_{\rm tot}^{\rm cryst}-\Sigma_i^N E_{\rm tot}^{\rm at})/N$ (where $E_{\rm tot}^{\rm cryst}$ is the total energy of crystal, $E_{\rm tot}^{\rm at}$ is the energy of constituent atoms, and N is the number of atoms in the unit cell of the compound). The comparison of $E_{\rm dif}$ for Ti_3SiC_2 and Ti_3SiC (Table V) shows that the introduction of the C-sublattice vacancy lowers $E_{\rm dif}$ (by ~0.03 Ry/atom). This may cause destabilization of the silicocarbide hexagonal structure and may quantitatively explain the absence of the homogeneity region (in the carbon sublattice) for Ti_3SiC_2.[6,8–10]

C. Solid solutions Ti_3SiCN and Ti_3SiCO

The TDOS and LDOS of the Ti_3SiCN and Ti_3SiCO solid solutions are shown in Figs. 13 and 14; some parameters of their electronic spectrum and charge distributions are given in Tables III and V. Taking into account that the main effects of the Ti-C chemical bonding in Ti_3SiC_2 are determined by the nearest neighbors, it is instructive to compare the data

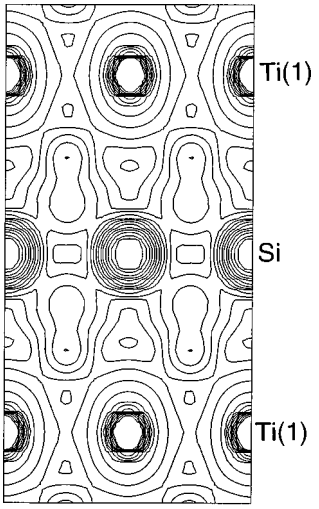

FIG. 8. Valence electron densities in Ti(1)-Si-Ti(1) layers of Ti_3SiC_2.

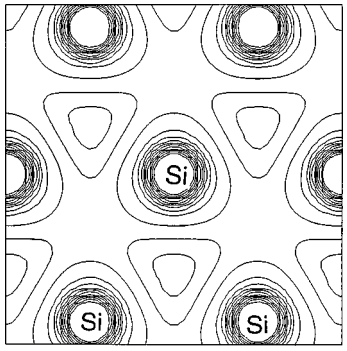

FIG. 9. Valence electron densities in Si-containing plane nets in the structure of Ti_3SiC_2.

obtained for Ti_3SiCN with the results for titanium carbonitrides (TiC_xN_{1-x}) and the hypothetical $B1$ solid solutions (SS's) in the Ti-Si-N-C system, for which C and N atoms also retain the octahedral environment. TiC_xN_{1-x} solid solutions have been studied by the relativistic KKR-average T-matrix technique,[28] as well as in the framework of the tight-binding-CPA (Ref. 29) and KKR-CPA (Ref. 30) methods. All the above-mentioned studies assume a random distribution of C and N atoms over the metalloid sublattice.[31] Long-range ordered model structures (supercells $Ti_4C_xN_{4-x}$; $x=0.1-4.0$) were employed to calculate TiC_xN_{1-x} by the LMTO (Ref. 25) and LAPW (Ref. 29) methods. Metastable $B1$ $TiSi_xN_yC_z$ SS's were simulated by the LMTO-ASA method in Ref. 32.

It follows from Fig. 13 that the formation of Ti_3SiCN is accompanied by noticeable changes in the spectrum of valence states caused primarily by the appearance of N $2s$ (not shown in Fig. 13) and N $2p$ subbands occurring with a narrowing of C $2s$ and C $2p$ subbands (as in the case of Ti_3SiC) and a decrease in the DOS. As a result, the p-d band of Ti_3SiCN is ~1.3 eV wider than the corresponding band of Ti_3SiC_2 and ~1.5 eV wider than that in Ti_3SiC. In previous calculations,[16,25,30] a nonmonotonic change in the width of the hybridized p-d band of TiC_xN_y (relative to TiC and TiN) was found, which is clearly seen also in the shape of the XPS

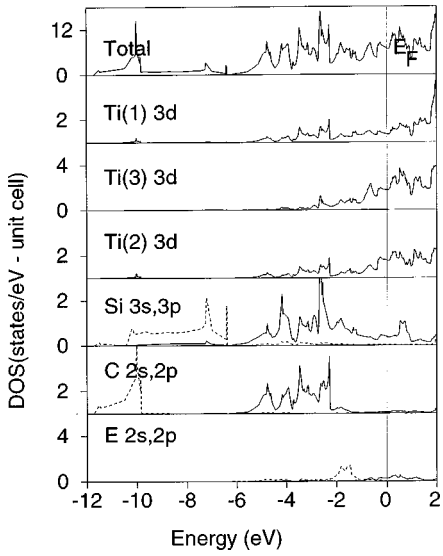

FIG. 10. Total and local DOS of nonstoichiometric Ti_3SiC.

TABLE IV. Core-level binding energies (eV) of Ti_3SiC_2 and some compounds in the Ti-Si-C system.

	Ti $2p_{3/2}$	Si $2p$	C $1s$
Ti	454.1		
TiC	454.8		281.9
Ti_5Si_3(O)	454.1	98.8	
$TiSi_xC_y$ ($B1$)	455.0	99.1	282.2
Ti_3SiC_2	454.9	99.5	282.1
Si		99.5	
SiC		100.4	282.3
SiO_2		103.1	

spectra, Fig. 15. As follows from our calculations, the tendencies in changing the valence spectrum are comparable for Ti_3SiC_2, Ti_3SiCN, and Ti_3SiN_2 and the TiC, TiC_xN_{1-x}, and TiN series. This points to the general similarity of interatomic interactions in titanium carbonitride and in Ti(3)-N-Ti(2)-C-Ti(1) layers of Ti_3SiCN.

On the other hand, the specific character of the crystal structure of Ti_3SiC_2 determines a considerable anisotropy in the interactions of structurally nonequivalent titanium atoms with nonmetal neighbors and with each other. As is seen from Fig. 13, d states of Ti(3) and Ti(2) atoms are concentrated in the energy region of the N $2p$ band, whereas the contributions from Ti(1) d states are negligibly small in this energy interval.

The maximum concentration of electron density is observed in the region of the hybridized p-d band for Ti(2) atoms participating in covalent N-Ti(2)-C bonds. The electron concentration for Ti(1) atoms, the main type of interaction for which there will be Ti(1)-C bonding, is smaller. Ti(3) atoms [Ti(3)-N bonds] are less bound with the metalloid sublattice (see also Fig. 16). Metal-metal interactions in (100) layers composed of Ti(1), Ti(2), and Ti(3) atoms are changed in the reverse sequence (Fig. 17): the growth of electronic density in ($dd\pi$) Ti-Ti bonding directions is clearly seen in the series Ti(2)<Ti(1)<Ti(3). According to

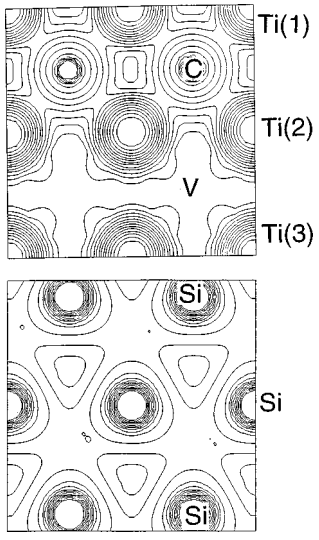

FIG. 11. Valence electron densities in Ti(3)-V-Ti(2)-C-Ti(1) and (100)Si layers of Ti_3SiC.

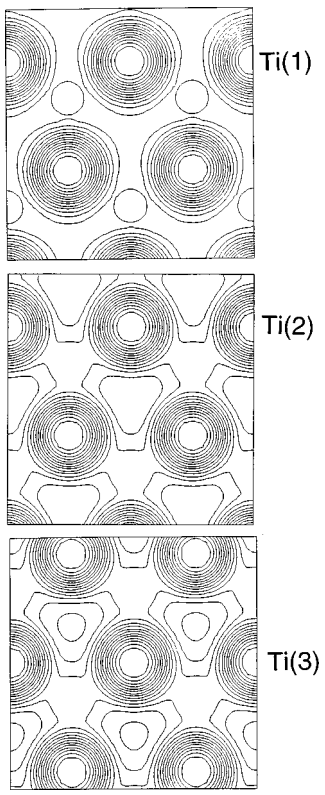

FIG. 12. Valence electron densities in (100) monolayers containing Ti(1)-Ti(3) atoms of Ti_3SiC.

the results obtained, the partial contributions to $N(E_F)$ are ~0.9 [Ti(1)] and 0.7 [Ti(2)] and ~1.9 states/eV unit cell [Ti(3)]. The bonding anisotropy of Ti atoms with nonmetal atoms and nonequivalent Ti atoms becomes more pronounced when oxygen atoms are introduced into the C sublattice of Ti_3SiC_2 (Figs. 14, 16, and 17).

The increase in the electron concentration from Ti_3SiCN to Ti_3SiCO is accompanied by a further increase in the occupation of the Ti t_{2g}-like band and an increase of $N(E_F)$ (Table V). Judging by the spatial distribution of the valence charge density (Fig. 17), metal-metal interactions become stronger in monolayers formed by Ti(2), Ti(1), and Ti(3) atoms, respectively, and in each case they are stronger than the corresponding metal-metal bonds in Ti_3SiCN. The contributions from d states of these Ti atoms to $N(E_F)$ in Ti_3SiCO are 1.2 [Ti(1)], 0.8 [Ti(2)], and 2.4 [Ti(3)] states/eV unit cell. In contrast to Ti_3SiCN, where C and N $2p$ bands overlap (it is possible to consider a common hybridized N $2p$–C $2p$–Ti $3d$ band), for Ti_3SiCO (Fig. 14) O $2p$ states are separated from the C $2p$–Ti $3d$ band by an energy gap (~1.47 eV), and in the range from −7.5 to −10 eV they are mixed with $3d$ states of Ti(2) and Ti(3) atoms. Investigating

TABLE V. TDOS at the Fermi level [$N(E_F)$, states/eV unit cell) and E_{dif} (Ry/atom) for Ti_3SiO_2- and Ti_3SiC_2-based solid solutions.

	Ti_3SiC_2	Ti_3SiC	Ti_3SiCN	Ti_3SiCO
$N(E_F)$	4.76	6.83	4.73	5.76
$-E_{dif}$	0.904	0.876	0.915	0.884

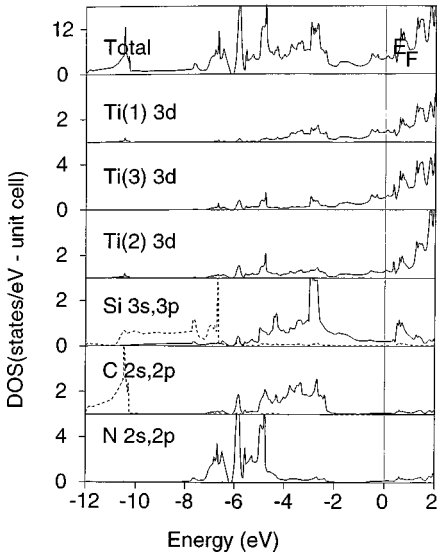

FIG. 13. Total and local DOS of Ti_3SiCN.

the physical-chemical properties of TiC_xN_{1-x}, some authors[33–37] note their nonmonotonic changes in the series $TiC \rightarrow TiC_xN_{1-x} \rightarrow TiN$. According to Ref. 33, the values of the Hall coefficient have a maximum for the SS's, and the minimum values of magnetic susceptibility are measured at a nitrogen concentration in the SS's of about 20 mol. %.

The concentration dependences of the bulk moduli for TiC_xN_{1-x}, as well as for some isostructural and isoelectronic SS's such as $Zr_xNb_{1-x}C$ and $Ti_xV_{1-x}C$, are of a considerable nonmonotonic character. The minimum of the heat capacity and the values of enthalpy for compositions close to $TiC_{0.7}N_{0.3}$ (Ref. 35) point to a relative strengthening of the chemical bonding for intermediate members of the series of TiC_xN_{1-x} SS's. Experiments studying the microhardness of these SS's, in which the maxima of microhardness were found for the compositions $TiC_{0.65}N_{0.28}$, $TiC_{0.5}N_{0.4}$, and $TiC_{0.8}N_{0.1}$,[36] may serve as circumstantial evidence that a relative strengthening of the chemical bonding takes place in TiC_xN_{1-x}. A qualitative explanation of this dependence was

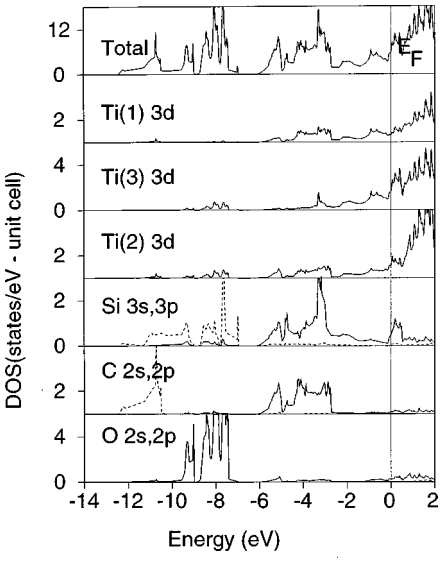

FIG. 14. Total and local DOS of Ti_3SiCO.

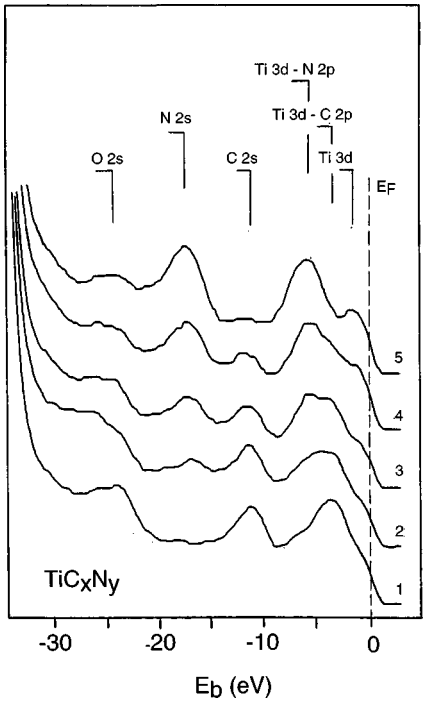

FIG. 15. XPS spectra of valence bands of SS's TiC_xN_y. 1, $TiC_{0.95}$; 2, $TiC_{0.7}N_{0.3}$; 3, $TiC_{0.5}N_{0.5}$; 4, $TiC_{0.3}N_{0.7}$; 5, $TiN_{0.93}$.

proposed in Ref. 37, where the change in microhardness of TiC_xN_{1-x} occurring with a variation of C/N was related to a decrease in the degree of dislocation mobility (owing to their blocking by interstitial atoms) and the formation of stronger metal-nonmetal bonds. Calculations of the deformation energy reveal that for TiC_xN_{1-x}, the maximum of microhardness should be at $x=0.4-0.6$, i.e., for SS's approximating those with equimolar composition.

An attempt to interpret the change of cohesive properties of TiC_xN_{1-x} SS's was made in the framework of the LMTO method.[16,25] The energy of alloy formation was calculated as

$$E_{af}(TiC_xN_{1-x}) = E_{coh}(TiC_xN_{1-x}) - xE_{coh}(TiC) - (1-x)E_{coh}(TiN).$$

Here $E_{af}(TiC_{0.5}N_{0.5})$ was obtained to be -16.55 kJ/mol, which shows that the formation of TiC_xN_{1-x} SS's is energetically favorable. Analogous calculations were performed for $B1$-$TiSi_xN_{1-x}$ SS's with partial replacement of N by C and O.[32] The energies of substitution, E_{sub}, for $TiSi_{0.125}N_{0.750}C_{0.125}$ and $TiSi_{0.125}N_{0.750}O_{0.125}$ were determined according to Ref. 16 to be equal to $+0.04$ and -0.05 Ry, respectively. Hence, oxygen impurities in N sites cause destabilization of the $B1$ lattice of SS's whereas in carbonitride SS's a reverse process should be observed. To our knowledge, no experimental data on synthesis and properties of Ti_3SiC_2-based SS's are available. According to our FLMTO calculations, maximum (absolute) value of E_{dif} in the series $Ti_3SiC_2 \rightarrow Ti_3SiCN \rightarrow Ti_3SiN_2$ has Ti_3SiCN (see Table V). In contrast, $|E_{dif}(Ti_3SiCO)| < |E_{dif}(Ti_3SiC_2)|$. Therefore, it can be inferred that the formation of carbonitride SS's based on Ti_3SiC_2 will cause an increase in their cohesive properties. Finally, the opposite situation should take place as a result of the oxidation of Ti_3SiC_2, where the

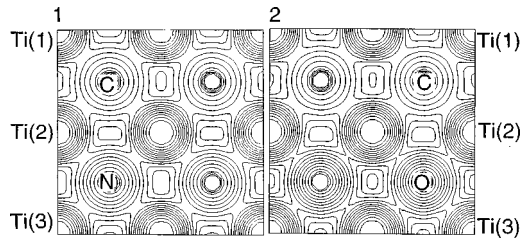

FIG. 16. Valence electron densities in (a) Ti(1)-C-Ti(2)-N-Ti(3) and Ti(1)-C-Ti(2)-O-Ti(3) and (b) layers of Ti_3SiCN and Ti_3SiCO.

partial substitution of C by O will initiate the destabilization of the crystal structure of hexagonal titanium silicocarbide.

IV. CONCLUSIONS

Using the first-principles self-consistent FLMTO method and x-ray photoelectron spectroscopy, we have studied the electronic structure and chemical bonding of the hexagonal Ti_3SiC_2 phase. It was shown that the interatomic interaction in the layers formed by Ti_6C octahedra is of a combined covalent-ionic-metallic type due to hybridization of C $2p$ and Ti $3d$ states, partial charge transfer in the direction Ti→C, and dd_π overlapping of metal states. The interatomic interaction in Si atom layers is determined mainly by the hybridization of Si $3p-$Si $3p$ states; the interaction with the layers made up of Ti_6C octahedra is relatively insignificant. This circumstance provides a qualitative explanation for the high plasticity of Ti_3SiC_2. A high density of electronic states was found at the Fermi level $[N(E_F)=4.8$ states/eV unit cell] which is responsible for metalliclike conducting properties of Ti_3SiC_2, as opposed to the care of TiC.

The tendencies of electronic distributions in C-Ti layers of silicocarbide SS's and the $B1$-TiC_xN_{1-x} and $TiSi_xN_yC_z$ SS's were found to change similarly. Finally, we conclude on the basis of total-energy estimates that the introduction of N atoms into the structure of Ti_3SiC_2 (formation of silicocarbonitride SS's) should lead to an increase in the cohesive properties of the system. By contrast, C vacancies and/or partial replacement C→O will cause a destabilization of the hexagonal lattice of the titanium siliconitride.

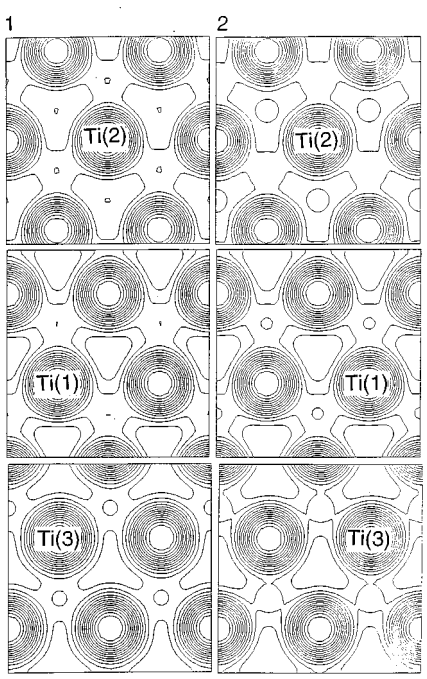

FIG. 17. Valence electron densities in (100) monolayers containing Ti(1), Ti(2), and Ti(3) atoms in SS's Ti_3SiCN (1) and Ti_3SiCO (2).

ACKNOWLEDGMENTS

The work at Northwestern University was supported by the U.S. Department of Energy (Grant No. DF-FG02-88ER45372) and by a grant of computing time on NERSC Supercomputers. The work in Russia was supported by RFFI Grant No. 96-03-32037.

[1] M. R. Jackson and R. L. Mehan, Ceram. Eng. Sci. Proc. **2**, 787 (1981).
[2] R. C. J. Schiepers, F. J. J. van Loo, and G. With, Am. Ceram. Soc. Bull. **71**, C-284 (1988).
[3] T. Yamamura, T. Ishikawa, M. Shibuya, T. Hisayuki, and K. Okamura, J. Mater. Sci. **23**, 2589 (1990).
[4] N. Muto, M. Miyayama, H. Yanagida, T. Kajiwava, N. Mori, H. Ishikawa, and H. Harada, J. Am. Chem. Soc. **73**, 443 (1990).
[5] B. Gottselig, E. Gyaramati, A. Naoumidis, and H. Nickel, J. Eur. Ceram. Soc. **6**, 153 (1990).
[6] H. J. Goldschmidt, *Interstitial Alloys* (Butterworth, London, 1967).
[7] J. C. Schuster, Ceram. Trans. **35**, 43 (1993).
[8] W. Jeitschko and H. Nowotny, Monatsh. Chem. **98**, 329 (1967).
[9] J. J. Nickel, K. K. Schweitzler, and P. Luxenberg, J. Less-Common Met. **26**, 335 (1972).
[10] T. Goto and T. Hirai, Mater. Res. Bull. **22**, 1195 (1987).
[11] R. Pompuch, J. Lis, L. Stobievski, and M. Tymkiewicz, J. Eur. Ceram. Soc. **5**, 283 (1989).
[12] J. Lis, R. Pampuch, J. Piekarczyk, and L. Stobievski, Ceram. Int. **19**, 219 (1993).
[13] L. Toth, *Carbides and Nitrides of Transition Metals* (Academic, London, 1971).
[14] Properties, *Synthesis and Application of Refractory Compounds*, edited by T. A. Kosolapova (Metallurgija, Moscow, 1986).
[15] P. Marksteiner, P. Redinger, and P. Weinberger, Z. Phys. B **62**, 443 (1986); B. M. Klein, D. A. Papaconstantopoulos, L. L. Boyer, A. Neckel, R. Zeller, and P. Dederichs, Phys. Rev. B **33**, 670 (1986); J. Redinger, R. Eibler, P. Herzig, A. Neckel, R. Podloucky, and E. Wimmer, J. Phys. Chem. Solids **47**, 387 (1986); J. Redinger, P. Marksteiner, and P. Weinberger, Z. Phys. B **63**, 321 (1986).
[16] V. A. Gubanov, A. L. Ivanovsky, and V. P. Zhukov, *Electronic Structure of Refractory Carbides and Nitrides* (Cambridge University Press, Cambridge, 1994).
[17] R. Pauling, *General Chemistry* (Freeman, San Francisco, 1970).
[18] M. Methfessel, C. O. Rodriguez, and O. K. Andersen, Phys. Rev. B **40**, 2009 (1989).

[19] L. Hedin and B. I. Lundqvist, J. Phys. C **4**, 2063 (1971).
[20] M. V. Kuznetsov, E. V. Shalaeva, S. V. Borisov, B. V. Mitrofanov, A. L. Ivanovsky, and G. P. Shveikin, Mendeleev Communications **3**, 110 (1995); M. V. Kuznetsov, E. V. Shalaeva, S. V. Borisov, B. V. Mitrofanov, and A. L. Ivanovsky, Thin Solid Films **279**, 75 (1996).
[21] A. Callenas, L. I. Johansson, N. A. Christensen, K. Schwartz, and P. Blacha, Phys. Rev. B **32**, 575 (1985); P. A. P. Lindberg and L. I. Johansson, Surf. Sci. **192**, 353 (1987).
[22] D. G. Kellerman, V. S. Gorshkov, Ya. N. Blinovskov, I. G. Grigorov, V. A. Perelyaev, and G. P. Shveikin, Inorg. Mater. **33**, 271 (1997).
[23] V. R. Galakhov, V. A. Trofimova, D. G. Kellerman, Ya. N. Blinovskov, and V. A. Perelyaev, in *Solid State Chemistry and Novel Materials Conference* (Academy of Sciences, Yekaterinburg, 1996), Vol. 1, p. 57.
[24] A. Neckel, Int. J. Quantum Chem. **23**, 1317 (1983).
[25] V. P. Zhukov, N. I. Medvedeva, and V. A. Gubanov, Phys. Status Solidi B **151**, 407 (1989).
[26] V. A. Gubanov, A. L. Ivanovsky, G. P. Shveikin, and D. E. Ellis, J. Phys. Chem. Solids **45**, 719 (1984).
[27] A. Neckel, in *The Physics and Chemistry of Carbides, Nitrides and Borides*, edited by R. Freer (Kluwer, Amsterdam, 1990), pp. 485–511.
[28] P. Weinberger, Phys. Status Solidi B **97**, 565 (); **98**, 207 (1980).
[29] J. Klima, J. Phys. C **15**, 689 (1982).
[30] J. Petru and J. Klima, Z. Phys. B **73**, 213 (1988).
[31] E. Gustenau-Michalek, P. Herzig, and A. Neckel, J. Alloys Compd. **73**, 213 (1995).
[32] A. L. Ivanovsky, N. I. Medvedeva, G. P. Shveikin, and V. M. Zhukovsky, Phys. Status Solidi B **195**, 195 (1996).
[33] L. B. Dubrovskaya, A. S. Borukhovich, I. I. Matveenko, G. P. Shveikin, and P. V. Geld, Fiz. Met. Metalloved. **32**, 555 (1971); L. B. Dubrovskaya, B. V. Mitrofanov, S. Z. Nazarova, and P. V. Geld, Phys. Status Solidi A **25**, K167 (1974).
[34] A. I. Avqustinnic, S. S. Ordanian, L. V. Kudryashova, and V. N. Fishev, Izv. Akad. Nauk SSSR, Neorg. Mater. **9**, 1358 (1973).
[35] A. G. Turchanin, S. A. Babenko, and I. I. Bilik, Izv. Akad. Nauk SSSR, Neorg. Mater. **20**, 1511 (1984); A. G. Turchanin and S. A. Babenko, Teplofiz. Vys. Temp. **20**, 887 (1982); A. G. Turchanin, S. A. Babenko, and V. S. Polishjuk, Zh. Strukt. Khim. **54**, 41 (1982).
[36] G. D. Bogomolov, G. P. Shveikin, S. I. Alamovsky, Yu. G. Zainulin, and V. D. Lubimov, Izv. Akad. Nauk SSSR, Neorg. Mater. **7**, 67 (1971); B. V. Mitrofanov, E. K. Plaksin, G. P. Shveikin, and V. D. Lubimov, *ibid.* **10**, 1001 (1974); T. Yamamoto, R. Kieffer, and P. Ettmayer, *8th Plansee Seminar* (Metallwork Plansee, Reutte, 1974), Vol. 4, p. 1; Yu. N. Vilk, Poroshkovaja Metallurg. **6**, 70 (1978) [Sov. Powder Metallurg. Metal Ceram. **17**, 467 (1978)].
[37] A. I. Gusev and G. P. Shveikin, Izv. Akad. Nauk SSSR, Neorg. Mater. **12**, 1565 (1976).